

Asymptotic solutions in forced convection turbulent boundary layers

Xia Wang and Luciano Castillo

Department of Mechanical, Aerospace and Nuclear Engineering,
Rensselaer Polytechnic Institute, Troy, NY 12180, USA
E-mail: castil2@rpi.edu

Received 6 September 2002
Published 6 March 2003

Abstract. A similarity analysis has been developed for a 2D forced convection turbulent boundary layer with and without a pressure gradient. Two new inner and outer temperature scalings are derived by means of similarity analysis of the equations of motion. The new scalings will be verified by the experimental data with adverse pressure gradient, favourable pressure gradient and zero pressure gradient respectively. It will be shown that the mean temperature profiles are dependent on the external pressure gradient and the upstream conditions. However, using the new scaling in inner variables or in outer variables, the temperature profiles collapse into a single curve. Thus, the true asymptotic solution for the temperature field exists even at a finite Péclet number. These results are confirmed by using the existing experimental data and compared with the results from various scalings. The asymptotic temperature profile or the self-similar profile found in the present analysis is in agreement with the fact that an asymptotic velocity profile exists if the mean velocity deficit profile is normalized by the Zagarola and Smits scaling (Zagarola and Smits 1998 *J. Fluid Mech.* **373** 33–79).

PACS numbers: 47.27.Te, 47.27.Ak, 47.27.Eq

JOT 4 (2003) 006

Contents

| | | |
|----------|--|----------|
| 1 | Introduction | 2 |
| 2 | The similarity analysis | 3 |
| 2.1 | Similarity analysis for the inner flow | 4 |
| 2.2 | Similarity analysis for the outer flow | 6 |
| 2.2.1 | The new outer temperature scaling. | 7 |
| 2.2.2 | Comparisons of the various outer scalings. | 8 |

| | | |
|----------|--|-----------|
| 3 | Experimental data | 8 |
| 4 | Results | 9 |
| 4.1 | The inner temperature profiles | 9 |
| 4.2 | Outer temperature profiles | 13 |
| 5 | Conclusion | 17 |

1. Introduction

Heat transfer in turbulent boundary layers plays a crucial role in industrial applications. For example, hot gases flowing over a turbine's cooler blade, air flowing over computer chips, etc, all involve the interaction of heat transfer and momentum transport between the fluid and the solid surface at different temperatures. It is of great interest to understand the physics of this interaction between scales for the temperature field and the velocity field, particularly the scales of the nonlinear turbulent quantities. In order to determine these scales, a similarity analysis will be applied to the equations of motion for a 2D, steady on the mean, incompressible flow with constant fluid properties.

Experiments on heat transfer in turbulent boundary layers are rather complex and difficult to control due to the interaction between the temperature field and the velocity field according to Kader [2]. Based on the Spalding analysis [3], the Reynolds analogy has been widely applied to investigate the heat transfer in turbulent boundary layers. By assuming an analogy between the heat transfer and momentum transport, a convenient approach has been established to study the forced convection turbulent boundary layer. However, the Reynolds analogy is a very rough method which breaks down when there is an external pressure gradient imposed in the outer flow, especially for an adverse pressure gradient (APG) flow. Moreover, many investigators, such as Blackwell *et al* [4] and Ayala *et al* [5] have shown that the turbulent Prandtl number, Pr_t , is not a constant across the turbulent boundary layer, especially for those flows subject to an external pressure gradient. This is contrary to the implications of the Reynolds analogy. Many advanced methods based on the Reynolds analogy have been proposed, and special efforts have been made to improve the turbulent Prandtl number Pr_t . However, there are no satisfying results yet, particularly in the scaling laws.

Similar to the standard law of the wall and the velocity defect law for the inner and outer velocity profiles in turbulent boundary layers, a thermal law of the wall and a thermal defect law have been presented for the inner and outer temperature profiles respectively [6]. However, the thermal law of the wall was born with the faults of the classical 'log-law'. For instance, there is only a single temperature scale for both the inner and outer flow. Furthermore, the thermal law of the wall cannot describe the thermal boundary layer subject to the APG according to Perry *et al* [7]. Also, it does not take into account the Péclet number, Pe , effects.

In 1966, Perry *et al* [7] presented an inverse half-power law for the temperature profile in the APG turbulent boundary layer using dimensionless analysis. However, this law cannot describe the heat transfer in the outer region of the boundary layer. In 1976, Perry and Hoffman [8] initially analysed the scaling for temperature fluctuations of the zero pressure gradient (ZPG) boundary layer. In 1991, Kader's investigation [2] made a significant contribution to this field. First, he considered the effect of Prandtl number, Pr , on the temperature profile. Second, two different scalings were proposed instead of one, as suggested in the classical approach for the inner and the

outer thermal boundary layer respectively. However, his analysis did not apply to a sharp variation of the wall temperature. Most recently, Volino and Simon [9] proposed a formulation for the velocity profile and the temperature profile in the turbulent boundary layer subject to a pressure gradient. They showed that their new formulation deviated from the standard law of the wall, but it was still in agreement with the experimental data studied. However, this agreement was only applicable for the inner thermal boundary layer region. Most of the previous investigations except those by Kader [2] and Perry *et al* [7] did not answer the question of how to scale the temperature profile. Instead they simply took the friction temperature, T_τ , as the temperature scale for both the inner and outer thermal boundary layer. Moreover, this single temperature scale approach failed to collapse the data in APG flows. In 1997, George *et al* [10] applied a similarity analysis to study the forced convection turbulent boundary layer. Two different scalings were proposed for both the inner and the outer temperature profiles respectively. However, their results were not verified for the pressure gradient (PG) boundary layer. More importantly, the effects of the PG and upstream conditions were not considered in their analysis. Therefore, the goal of this investigation is to apply the ‘equilibrium similarity analysis’ proposed by George and Castillo [11] and Castillo and George [12] to study forced convection turbulent boundary layers. Attention will be given to forced convection turbulent boundary layers with and without PG. Using the existing experimental data, comparisons of different scalings will be performed.

2. The similarity analysis

According to the similarity analysis for the turbulent boundary layer with ZPG proposed by George and Castillo [11] and with PG by Castillo and George [12], the scales for both the inner and outer flows are dictated by equations of motion and their boundary layer conditions alone. Since in the limit as $Re \rightarrow \infty$, the boundary layer equations become independent of Re ; therefore, any scale or function representing the boundary layer solutions must also be independent of the local Re . (This is the asymptotic invariance principle (AIP) proposed by George and Castillo [11].) Hence, in this limit, the inner and outer scales of the turbulent boundary layer will be determined.

Castillo and George [12] have shown that the outer mean deficit velocity profiles and the outer Reynolds shear stresses are scaled with U_∞ and $U_\infty^2 d\delta/dx$ respectively. Moreover, the Reynolds normal stresses in outer variables are scaled only with U_∞^2 . Using a similar approach to the inner momentum equation, it has been shown that the velocity profiles and Reynolds stresses are scaled with the friction velocity, u_τ and u_τ^2 respectively, which are the same as those in the classical theory. Therefore, the overlap region is characterized by two different velocity scales instead of one as suggested in the classical view.

A similar approach will be used here for the forced convection turbulent boundary layer in order to determine the scales for the temperature field and the corresponding constraints. The turbulent boundary layer under consideration is a 2D, steady state on the mean, incompressible flow with heat transfer between the wall and the free stream. The physical properties, such as density, ρ , kinematic viscosity, ν , and thermal diffusivity, a , are assumed to be constant within the small range of temperature difference studied here. Integrating the inner energy equation and applying the corresponding boundary layer conditions at the wall yield the integral form of the inner energy equation, which is given as

$$-\frac{q_w}{\rho c_p} = a \frac{\partial T}{\partial y} - \langle tv \rangle. \quad (1)$$

The outer energy equation is given by

$$U \frac{\partial T}{\partial x} + V \frac{\partial T}{\partial y} = \frac{\partial}{\partial y} [-\langle tv \rangle]. \quad (2)$$

The related boundary layer conditions are

$$y \rightarrow 0, T \rightarrow T_w; \quad \langle tv \rangle \rightarrow 0; \quad a \frac{\partial T}{\partial y} \Big|_{y=0} = -\frac{q_w}{\rho c_p}; \quad (3)$$

$$y \rightarrow \infty, T \rightarrow T_\infty; \quad \langle tv \rangle \rightarrow 0. \quad (4)$$

The above equations can describe the energy transport in the turbulent boundary layer exactly in the limit as $Pe \rightarrow \infty$ [13].

2.1. Similarity analysis for the inner flow

Solutions for the inner thermal profiles and the inner turbulent heat flux are sought of the following forms:

$$T_w - T = T_{si}(x) g_{si}(y_T^+, \delta_T^+, Pr, *) \quad (5)$$

$$-\langle tv \rangle = F_{si}(x) h_{si}(y_T^+, \delta_T^+, Pr, *) \quad (6)$$

where $T_{si}(x)$ and $F_{si}(x)$ are the unknown inner temperature scale and inner turbulent flux scale respectively, which will be determined from the inner energy equation and its boundary layer conditions. The variables inside the similarity functions g_{si} and h_{si} represent the inner similarity length scale, y_T^+ , the local Péclet number dependence, δ_T^+ , the Prandtl number, Pr , and any possible dependence on the upstream conditions, $*$.

The Stanton number is defined as $St = (q_w / \rho C_p U_\infty (T_w - T_\infty))$, and the skin friction coefficient is defined as $C_f / 2 = \tau_w / \rho U_\infty^2$. Notice that the heat flux on the wall, q_w , in the thermal boundary layer corresponds to the wall shear stress, τ_w , in the momentum boundary layer. Therefore, the Stanton number is very similar to the skin friction coefficient. However, the Stanton number and the skin friction coefficient behave very differently with the change of strength of PG in the outer flow, which has been presented by Blackwell *et al* [4] for APG flow and Kays and Crawford [14] for favourable pressure gradient (FPG) flow. For instance, for a strong APG flow, the skin friction decreases with increasing strength of PG. Nonetheless, the Stanton number will increase slightly provided that the heat flux on the wall is constant. In the similarity analysis of the momentum equation, the inner length scale y^+ can be written in terms of the skin friction coefficient and free stream velocity as

$$y^+ = \frac{U_\tau y}{\nu} = \frac{U_\infty y}{\nu} \sqrt{\frac{C_f}{2}}. \quad (7)$$

Hence when choosing the length scale y_T^+ for the inner energy equation, the Stanton number will be used to take the place of the skin friction coefficient as

$$y_T^+ = \frac{U_\infty y}{\nu} \sqrt{St}, \quad (8)$$

which is a reasonable assumption since the Stanton number includes all the heat transfer information.

In the limit as $Pe \rightarrow \infty$, the similarity solutions of equations (5) and (6) are independent of the local Péclet number, δ_T^+ , as required by the AIP. Thus, equations (5) and (6) reduce to

$$T_w - T = T_{si}(x)g_{si\infty}(y_T^+, Pr, *) \quad (9)$$

$$-\langle vt \rangle = F_{si}(x)h_{si\infty}(y_T^+, Pr, *) \quad (10)$$

where $g_{si\infty}$ and $h_{si\infty}$ are the asymptotic profiles for the mean temperature and the turbulent heat flux respectively. Notice that the upstream conditions, $*$, have been retained here because they may influence the shape of the profiles even in this limit. Substituting these asymptotic similarity solutions into the inner energy equation (1), the inner energy equation is written in similarity form as

$$\left[U_\infty T_{si} \frac{a}{\nu} \sqrt{St} \right] g_{si\infty} + [F_{si}] h_{si\infty} = \left[-\frac{q_w}{\rho c_p} \right]. \quad (11)$$

Full similarity exists only if all the terms in the square brackets have the same x dependence; therefore, they must evolve together. In other words, they must be proportional to each other, such as

$$\left[U_\infty T_{si} \frac{a}{\nu} \sqrt{St} \right] \sim [F_{si}] \sim \left[-\frac{q_w}{\rho c_p} \right]. \quad (12)$$

Consequently, the scales for the inner mean temperature and the inner turbulent heat flux are given as

$$T_{si} = Pr \sqrt{St} (T_w - T_\infty), \quad (13)$$

$$F_{si} = -\frac{q_w}{\rho c_p}. \quad (14)$$

Obviously, the inner temperature scale is different from the classical scale. In the classical method, analogous to the friction velocity, u_τ , the inner mean temperature scale is given by the friction temperature, T_τ , defined as

$$T_\tau = \frac{q_w}{\rho c_p u_\tau}, \quad (15)$$

and the inner length scale is given as

$$y^+ = \frac{y u_\tau}{\nu}. \quad (16)$$

The friction velocity in the above equations is determined from the wall shear stress as $u_\tau^2 = \tau_w / \rho$. This is indeed the Reynolds analogy of the law of the wall, but it breaks down when an external PG is imposed on the flow. George *et al* [10] used a similar analysis as the one mentioned above. However, they adopted a different inner length scale and therefore obtained a different temperature scale. Here we call this the George–Wosnik–Castillo (GWC) scaling to make reference to the authors. Table 1 shows the comparison of various results for the inner temperature scaling from various investigations. The first row represents the classical scaling using Reynolds analogy, the second row shows the GWC scaling using similarity analysis and the last row shows the scaling from the present analysis. Notice that both the inner length scale and the inner temperature scale are different for all three theories. In addition, it is obvious that the inner temperature scaling of the new theory contains the effects of the Prandtl number and the Stanton number. A comparison between these scales will be shown in the subsequent sections.

Table 1. The comparisons of different inner temperature scalings.

| Theory | Inner similarity length scale y_T^+ | Inner temperature scale: T_{si} |
|------------------|--|---|
| Reynolds analogy | $y_T^+ = y^+ = \frac{yu_\tau}{\nu}$ | $T_{si} = T_\tau = \frac{q_w}{\rho C_p u_\tau}$ |
| GWC | $y_T^+ = \frac{yq_w/\rho C_p}{\alpha(T_w - T_\infty)}$ | $T_{si} = T_w - T_\infty$ |
| Present analysis | $y_T^+ = \frac{yU_\infty}{\nu} \sqrt{St}$ | $T_{si} = Pr(T_w - T_\infty) \sqrt{St}$ |

2.2. Similarity analysis for the outer flow

The outer scales for the temperature defect and the turbulent heat flux can be determined using the similarity analysis of the outer boundary layer equations. The outer solutions of the energy equation can be sought in the forms of

$$T - T_\infty = T_{so}(x)g_{so}(\bar{y}_T, \delta_T^+, Pr, *) \quad (17)$$

$$-\langle vt \rangle = F_{so}(x)h_{so}(\bar{y}_T, \delta_T^+, Pr, *) \quad (18)$$

where $\bar{y}_T = y/\delta_T$ is the outer similarity length scale and δ_T is the outer length scale, which could be defined in terms of the thermal boundary layer thickness or the enthalpy thickness. The similarity functions g_{so} and h_{so} are the outer temperature profile and the turbulent heat flux profile, respectively. The arguments inside the functions g_{so} and h_{so} represent the local Péclet number dependence given by δ_T^+ , the local Prandtl number, Pr , effects and any possible dependence on the upstream conditions $*$. The unknown outer temperature scale and the unknown outer turbulent heat flux scale are given as T_{so} and F_{so} , respectively. These unknown scales depend on x only and must be determined from the outer thermal equation.

In the limit as $Re \rightarrow \infty$ or $Pe \rightarrow \infty$, the momentum equation and the energy equation are independent of Re or Pe as required by AIP. Hence, in this limit, the outer solution forms of the energy equation are reduced to

$$T - T_\infty = T_{so}(x)g_{so\infty}(\bar{y}_T, Pr, *) \quad (19)$$

$$-\langle vt \rangle = F_{so}(x)h_{so\infty}(\bar{y}_T, Pr, *), \quad (20)$$

where the ∞ is used to represent the asymptotic profiles of $g_{so\infty}$ and $h_{so\infty}$, which are independent of Re or Pe . Notice that the upstream dependence has been retained because the flow may depend on it even in this limit.

Also, similar forms exist for the velocity deficit profile and the Reynolds shear stress profile given as

$$U_\infty - U = U_{so}(x)f_{op\infty}(\bar{y}, \Lambda; *) \quad (21)$$

$$-\langle uv \rangle = R_{so}(x)r_{op\infty}(\bar{y}, \Lambda; *), \quad (22)$$

where $U_{so} = U_\infty$ and $R_{so} = U_\infty^2 d\delta/dx$ have been determined by the similarity analysis of Castillo and George [12]. Substituting these asymptotic similarity solutions of equations (19)–(22) into the outer energy equation (2), and using the continuity equation to get the V component,

the outer energy equation is written in the similarity form as

$$\begin{aligned} \left[\frac{\delta_T}{T_{so}} \frac{dT_{so}}{dx} \right] (1 + f_{op\infty}) g_{so\infty} - \left[\frac{d\delta_T}{dx} \right] \bar{y}_T (1 + f_{op\infty}) g'_{so\infty} \\ - \left[\frac{\delta}{U_\infty} \frac{dU_\infty}{dx} \right] \bar{y} \left(1 + \int_0^{\bar{y}} f_{op\infty} d\tilde{y} \right) g'_{so\infty} \\ + \left[\frac{d\delta}{dx} \right] \bar{y} \left(f_{op\infty} + \int_0^{\bar{y}} f_{op\infty} d\tilde{y} \right) g'_{so\infty} = \left[\frac{F_{so}}{U_\infty T_{so}} \right] h'_{so\infty}. \end{aligned} \quad (23)$$

As in the inner similarity analysis, the terms in the square brackets depend on x , and full similarity exists only if those terms have the same x dependence. Consequently, they must be proportional to each other. Thus,

$$\frac{\delta_T}{T_{so}} \frac{dT_{so}}{dx} \sim \frac{\delta}{U_\infty} \frac{dU_\infty}{dx} \sim \frac{d\delta_T}{dx} \sim \frac{d\delta}{dx} \sim \frac{F_{so}}{U_\infty T_{so}}. \quad (24)$$

Taking the similarity of the last two terms yields

$$F_{so} \sim U_\infty T_{so} \frac{d\delta}{dx}. \quad (25)$$

Matching the inner and outer heat flux and Reynolds shear stress in the limit as $Pe \rightarrow \infty$, the outer temperature scale can be obtained as

$$T_{so} \sim \frac{St}{C_f/2} (T_w - T_\infty) \quad (26)$$

which has been shown by George *et al* [10]. Notice that this new outer scaling was obtained in the limit as $Pe \rightarrow \infty$ or $Re \rightarrow \infty$. In this limit, the flow loses its dependence on Re or Pe . Therefore, at finite Re or Pe , the temperature profiles should not be expected to collapse to one single curve. In addition, the flow may still be affected by the upstream conditions even in this limit. Now it will be of great interest to look for the real asymptotic solution so that the effects of the upstream condition and Reynolds number dependence can be removed even if at finite Reynolds number or Péclet number.

2.2.1. The new outer temperature scaling. Zagarola and Smits [1] have shown that the outer velocity scaling for the pipe flow is $U_\infty \delta^*/\delta$. Later on, Castillo [15] got exactly the same outer velocity scaling for the PG turbulent boundary layer using similarity analysis. He showed that this new velocity scaling could remove the effects of the different upstream conditions, Reynolds number dependence, and the PG effects on the outer flow. Thus, the true asymptotic velocity profile for the ZPG, APG and FPG flow was found. Now the attention will be focused on seeking the proper outer temperature scaling such that the true asymptotic temperature profile is found.

We assume that the outer temperature deficit profile of equation (17) can be rewritten as

$$T - T_\infty = \tilde{T}_{so}(x, \delta_T^+, *) \tilde{g}_{so\infty}(\bar{y}_T). \quad (27)$$

The new unknown temperature scale, \tilde{T}_{so} , needs to be determined using similarity analysis, and $\tilde{g}_{so\infty}$ represents the true asymptotic temperature function. Notice that the new unknown temperature scale \tilde{T}_{so} includes the effects of upstream conditions and Péclet number, and $\tilde{g}_{so\infty}$ depends on \bar{y}_T only.

The so-called thermal displacement thickness, δ_T^* , is defined as

$$\delta_T^* = \int_0^\infty \frac{T - T_\infty}{T_w - T_\infty} dy. \quad (28)$$

Substituting equation (27) into the definition of the thermal boundary layer thickness, it follows that

$$\left[\frac{\delta_T^*}{\delta_T} \right] = \left[\frac{\tilde{T}_{so}(x, \delta^+, *)}{T_w - T_\infty} \right] \int_0^1 \tilde{g}_{so\infty} d\bar{y}_T. \quad (29)$$

For the similarity solutions to exist, the bracketed terms should have the same x dependence, thus,

$$\frac{\delta_T^*}{\delta_T} \sim \frac{\tilde{T}_{so}(x, \delta^+, *)}{T_w - T_\infty}. \quad (30)$$

Hence the new outer temperature scaling is given as

$$\tilde{T}_{so}(x, \delta^+, *) = (T_w - T_\infty) \frac{\delta_T^*}{\delta_T}. \quad (31)$$

Interestingly, this outer temperature scaling is very similar to the outer Zagarola/Smits velocity scaling $U_\infty \delta_* / \delta$, and should contain the effects of the unknown upstream conditions and the Péclet number effect as well. Then, the true asymptotic temperature profile should exist if this new temperature profile scale is correct.

2.2.2. Comparisons of the various outer scalings. As mentioned previously, the outer scaling in the classical view is determined using the Reynolds analogy. Since in the classical theory a single velocity scaling is assumed, the mean velocity deficit profiles are normalized by the friction velocity, given as

$$\frac{U_\infty - U}{u_\tau}(x) = f_o(\bar{y}). \quad (32)$$

Therefore, in a similar manner, the outer mean temperature profiles are normalized by the inner friction temperature, T_τ , given by

$$\frac{T_\infty - T}{T_\tau}(x) = f_o(\bar{y}_T) \quad (33)$$

where T_τ is given as $q_w / \rho C_p u_\tau$. Table 2 summarizes the outer temperature scaling from various theories. The first row shows the classical scaling by Reynolds analogy, the second row shows the results from the similarity analysis of GWC and the third row shows the new scaling from the present investigation. The outer length scale is the same for all three theories, whereas the temperature scales are quite different from each other.

3. Experimental data

Different experimental data will be used to compare the classical scaling, the GWC scaling and the current scaling for both the inner and the outer temperature profiles. Here, we include the ZPG experimental data of Blackwell *et al* [4] and the ZPG data of Blom [16] with two different free stream speeds of 6 and 10 m s⁻¹ (fixed upstream conditions). For the measurements by Blom [16], the first 1 m of the test section was not heated, while at the leading edge the boundary

Table 2. The comparisons of different outer temperature scales.

| Theory | Outer similarity length scale: \bar{y}_T | Outer temperature scale: $T_{so}(x)$ |
|------------------|--|---|
| Reynolds analogy | $\bar{y}_T = \frac{y}{\delta_T}$ | $T_{so} = T_\tau = \frac{q_w}{\rho C_p u_\tau}$ |
| GWC | $\bar{y}_T = \frac{y}{\delta_T}$ | $T_{so} = (T_w - T_\infty) \frac{St}{C_f/2}$ |
| Present analysis | $\bar{y}_T = \frac{y}{\delta_T}$ | $T_{so} = (T_w - T_\infty) \frac{\delta_T^*}{\delta_T}$ |

layer was tripped using a tripping wire of cylindrical shape with a diameter of 3 mm. Thus, the momentum boundary layer begins earlier than the thermal boundary layer, which will affect the temperature profile in the outer region as shown in subsequent sections. Meanwhile, we study the APG experimental data of Orlando *et al* [17] with a PG power of $m = -0.275$ and Blackwell *et al* [4] with $m = -0.2$ and -0.15 . These APG experiments were performed such that a power relationship between the free stream velocity and the streamwise distance exists, $U_\infty \sim x^m$, where the power coefficient, m , represents the strength of the PG. The experimental data from Orlando *et al* [17] have a power coefficient $m = -0.275$, and therefore the strongest APG, followed by those of Blackwell *et al* [4] with $m = -0.2$ and -0.15 . In addition, each experimental data has almost the same fixed wind tunnel speed, U_o (upstream conditions), of 9.74, 10.1, 11.1 m s^{-1} for Blackwell *et al* [4] with $m = 0, -0.15$ and -0.2 respectively. The strong APG data of Orlando *et al* [17] have a fixed wind tunnel speed U_o of 11.6 m s^{-1} . The maximum Reynolds number based on the momentum thickness, R_θ , achieved from the data considered in this investigation is about 3000, while the lowest is around 550.

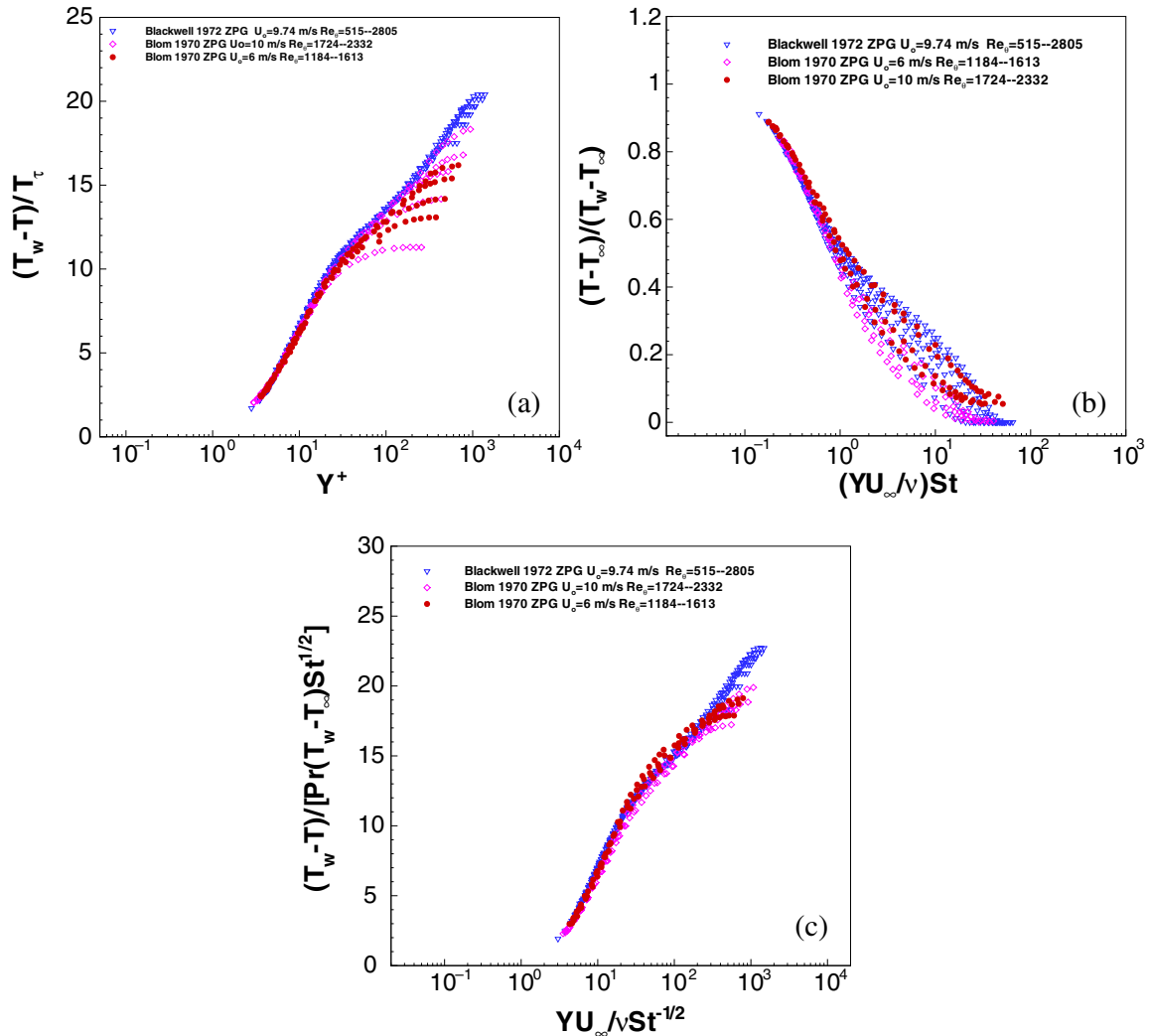
Furthermore, Thielbahr *et al* [18] provided the temperature data for the FPG turbulent boundary layer with $0 \leq K \leq 1.45 \times 10^{-6}$ (K is a PG parameter, defined as $(\nu/U_\infty^2)(dU_\infty/dx)$, where $K > 0$ denotes acceleration). The upstream speed is 12.45, 10.34 and 7.5 m s^{-1} for the corresponding K of 0.57×10^{-6} , 0.77×10^{-6} and 1.45×10^{-6} respectively. A 9.525 mm wide strip of coarse grit garnet paper (carborundum type 50) was used to trip the flow to form the turbulent boundary layer.

4. Results

Comparisons among the three different scalings in inner and outer variables for the ZPG, FPG, and APG forced convection flow will be made herein. The effects of the PG and upstream conditions will be analysed using the existing data.

4.1. The inner temperature profiles

Figure 1 shows the inner temperature profiles in semi-log scale for all the ZPG data discussed above. Note that the data have different upstream conditions (i.e. in this case wind tunnel speed). Figure 1(a) shows the profiles normalized by the classical scaling. Figure 1(b) shows the same ZPG experimental data, but these data are now normalized by the GWC scaling. Figure 1(c) shows the profiles normalized by the new scaling. Notice that using the new inner scaling, the profiles collapse into one single curve, regardless of the difference in the upstream speeds. Moreover, the classical scaling collapses the data better than the GWC scaling.



JOT 4 (2003) 006

Figure 1. Comparisons of different inner scalings for the ZPG flow. (a) Scaling using Reynolds analogy. (b) Scaling using the GWC analysis. (c) Scaling from the present analysis.

Figure 2 shows the APG experimental data of Orlando *et al* [17] and Blackwell *et al* [4] in semi-log scale. Clearly, the new scaling shown in figure 2(c) collapses the data into a single curve. Furthermore, the new scaling successfully removes the effects of the external PGs and the upstream conditions. The success of this scaling is more evident for the APG data than for the ZPG data. In addition, notice that the Reynolds analogy fails to collapse the APG data as shown in figure 2(a). Furthermore, using the classical scaling, it is clear that the temperature profiles collapse for a given set of upstream conditions (such as wind tunnel speed) and for a given strength of PG, but these profiles collapse to a different curve. In addition, the collapse of the profiles using the GWC scaling is far better than using the classical scaling, but it is less satisfying than using the present scaling. Consequently, it means that at least for APG flows without separation, the inner flow is independent of the PG. In fact, Castillo [19] showed that as

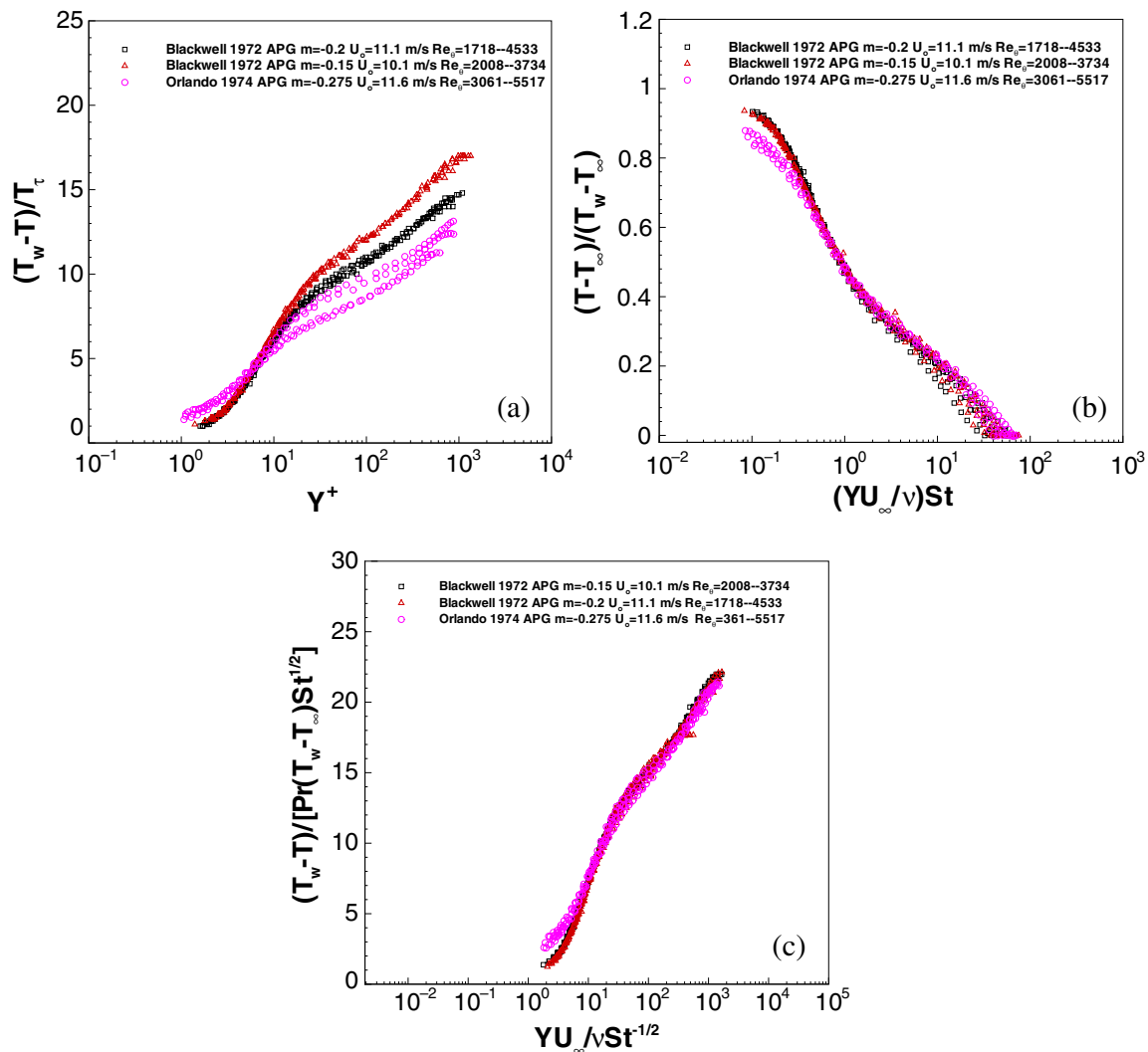


Figure 2. Comparisons of different inner scalings for the APG flow. (a) Scaling using Reynolds analogy. (b) Scaling using the GWC analysis. (c) Scaling from the present analysis.

long as the boundary layer did not approach the separation point, the inner flow was not affected by the external PG.

Obviously, the similarity analysis presented here works very well for the ZPG and APG turbulent boundary layer with heat transfer. Subsequently, it should work for the FPG turbulent boundary layer as well. Figure 3 shows Thielbahr *et al*'s FPG data using the three different scalings mentioned before. Clearly, using the new scaling as shown in figure 3(c), the data collapse better than using the other two scalings as shown in figures 3(a) and (b). However, for the FPG data, the advantages of the new scaling are not as obvious as for the ZPG data and APG data, which may be explained by the measurements themselves. First, notice that for this measurement, the pressure parameter K , defined as $(\nu/U_\infty^2)(dU_\infty/dx)$, is changing from 0.57×10^{-6} to 1.45×10^{-6} . Second, the upstream velocity varies from 7.5 to 12.45 m s $^{-1}$.

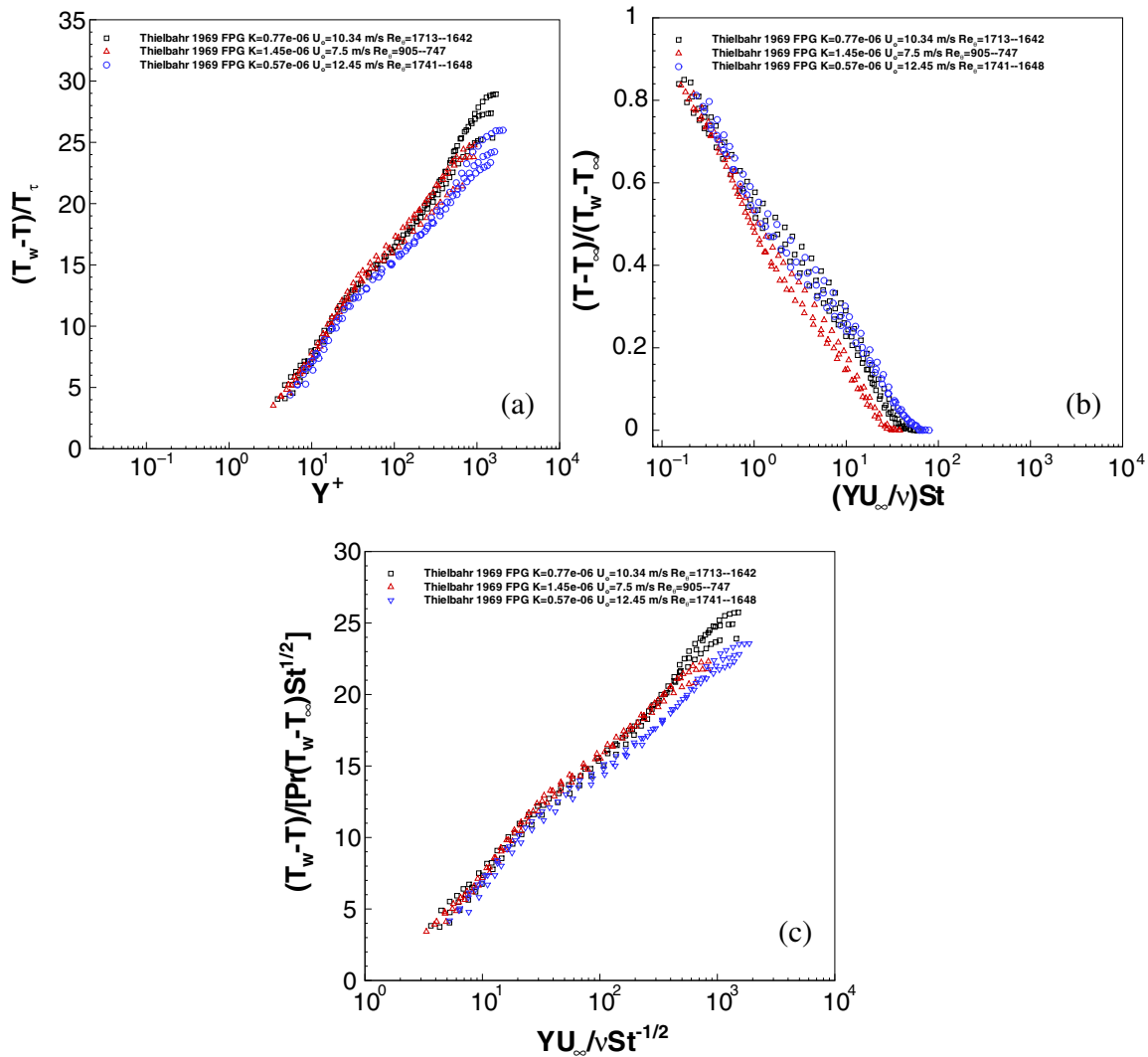


Figure 3. Comparisons of different inner scalings for the FPG flow. (a) Scaling using Reynolds analogy. (b) Scaling using the GWC analysis. (c) Scaling from the present analysis.

In addition, for this experiment, only the thermal data were measured, while the hydrodynamic data were interpolated from Julien's experiment [20], which involved isothermal FPG flows only under the same test conditions. Furthermore, the boundary layer in the FPG flow is very thin compared with one in the ZPG or APG flow, which thus makes it more difficult to obtain accurate results.

Figure 4 combined ZPG experimental data of figure 1, APG data of figure 2 and FPG data of figure 3. As before, the classical scaling profiles are shown in figure 4(a) while the GWC scaling is shown in figure 4(b). The data show an obvious dependence on the PG and the upstream conditions using the classical scaling or the GWC scaling. However, using the new scaling as shown in figure 4(c), all the data nearly collapse into one single curve, regardless of the

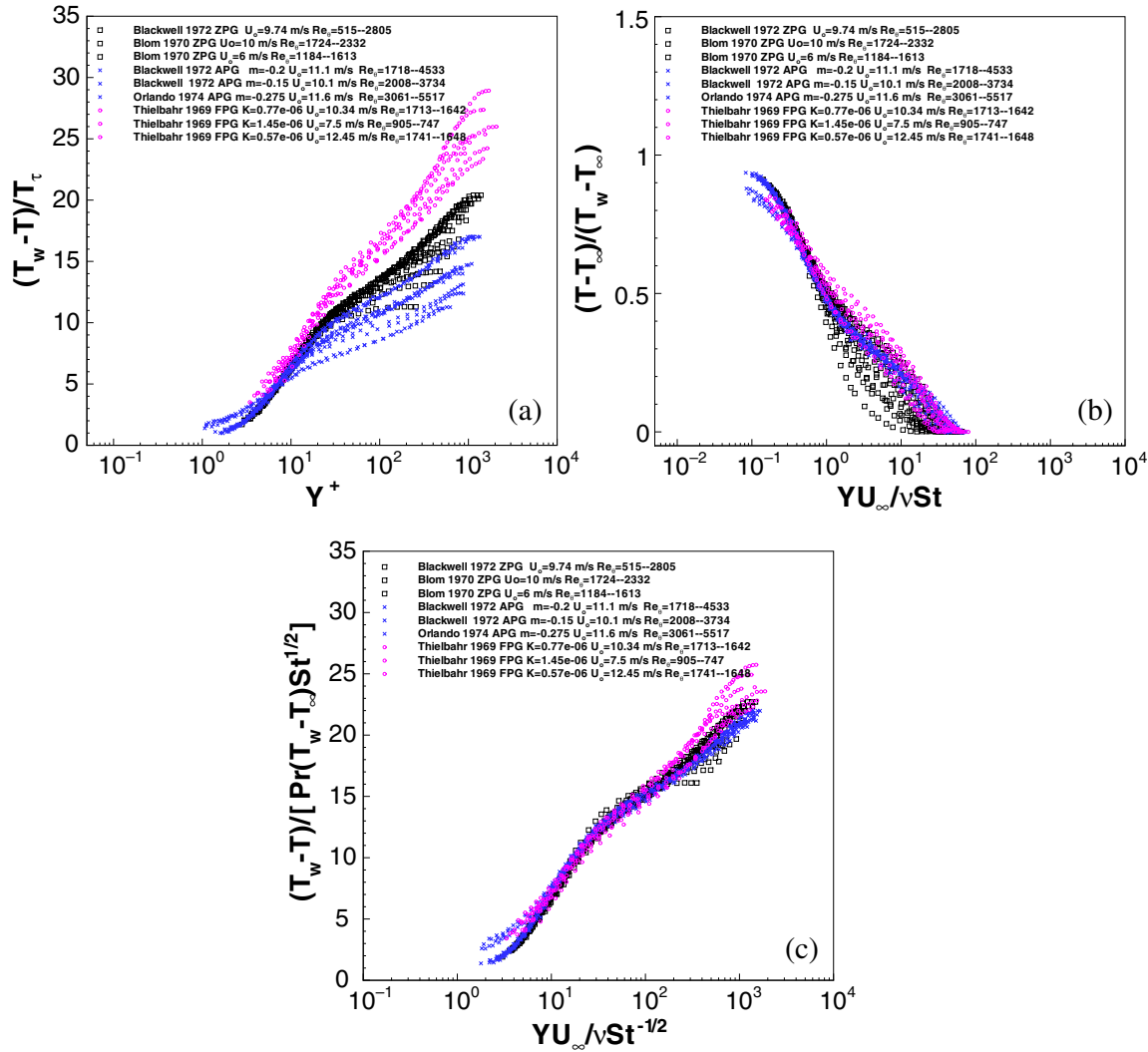


Figure 4. Comparisons of different inner scalings for the ZPG, APG and FPG flow. (a) Scaling using Reynolds analogy. (b) Scaling using the GWC analysis. (c) Scaling from the present analysis.

strength of the PG and the upstream conditions. Therefore, it is possible to find the asymptotic profile sought in the previous sections at finite Reynolds number, but only when the profiles are normalized with the new scaling.

4.2. Outer temperature profiles

The ZPG experimental data of Blackwell *et al* [4] and Blom [16] shown in figure 1 are now normalized in outer variables using the classical scaling, the GWC scaling, and the new scaling as shown in figures 5(a)–(c) respectively. Notice that using the classical scaling and the GWC scaling, the data of Blom [16] with a fixed wind tunnel speed of 10 and 6 m s⁻¹ cannot collapse

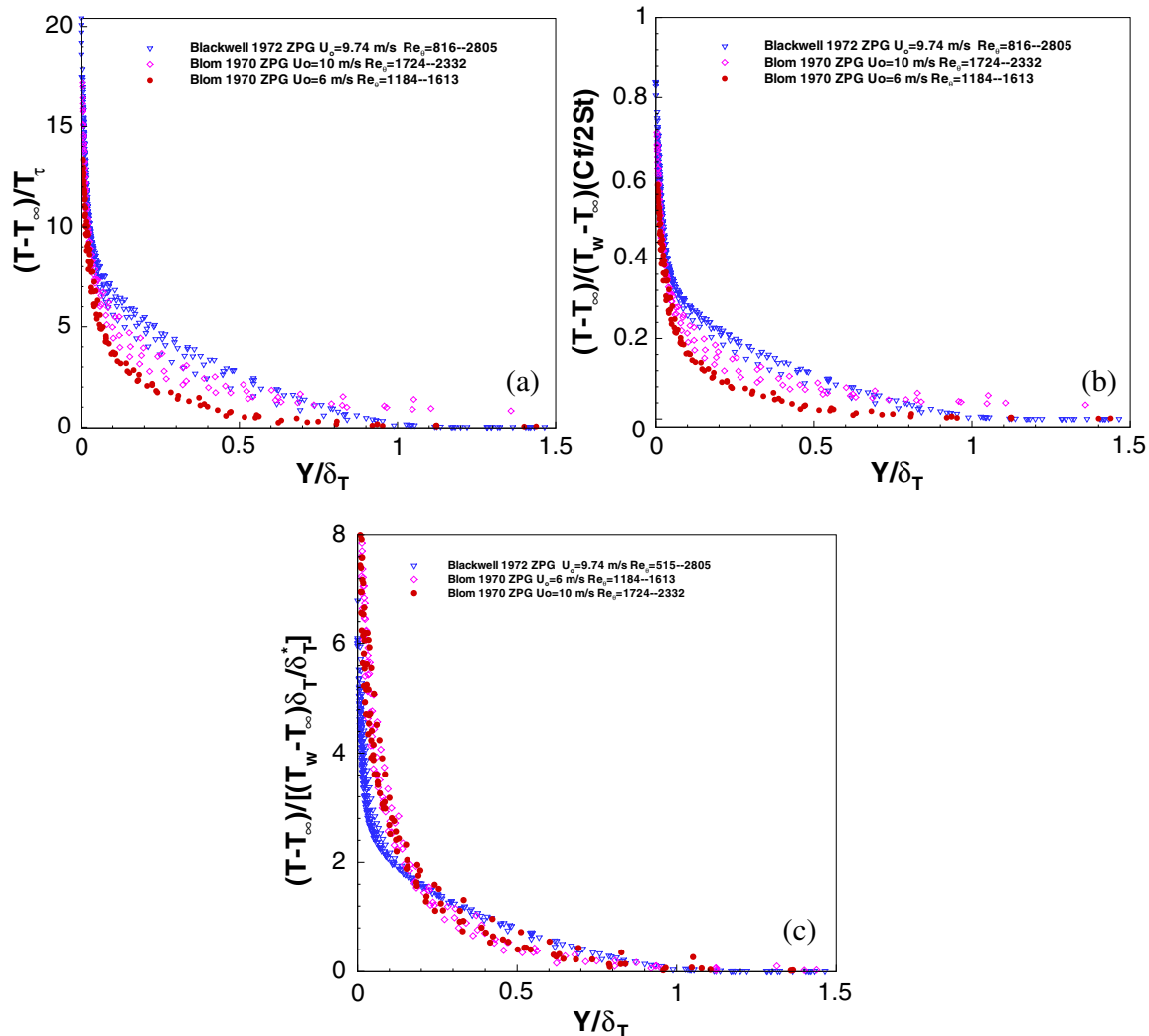


Figure 5. Comparisons of different outer scalings for the ZPG flow. (a) Scaling using Reynolds analogy. (b) Scaling using the GWC analysis. (c) Scaling from the present analysis.

into a single curve. However, using the new scaling, these two experimental data collapse, but to a different curve from the profile of the Blackwell *et al* ZPG [4]. This could be explained by the fact that for the experimental data of Blom [16], the thermal boundary layer develops later than the momentum boundary layer. The delay for the thermal boundary layer therefore affected the outer temperature profile, which has been presented by Kays and Crawford [14].

Figure 6 includes all the APG experimental data of Blackwell *et al* [4] and Orlando *et al* [17]. Clearly, the profiles using the classical scaling or the GWC scaling collapse the experimental data but to different curves, depending on the strength of the external PG. However, using the new scaling shown in figure 6(c), the profiles collapse into a single curve regardless of the strengths of the PG and the upstream conditions. Thus, the outer asymptotic profile for APG flows is found even at finite Reynolds number.

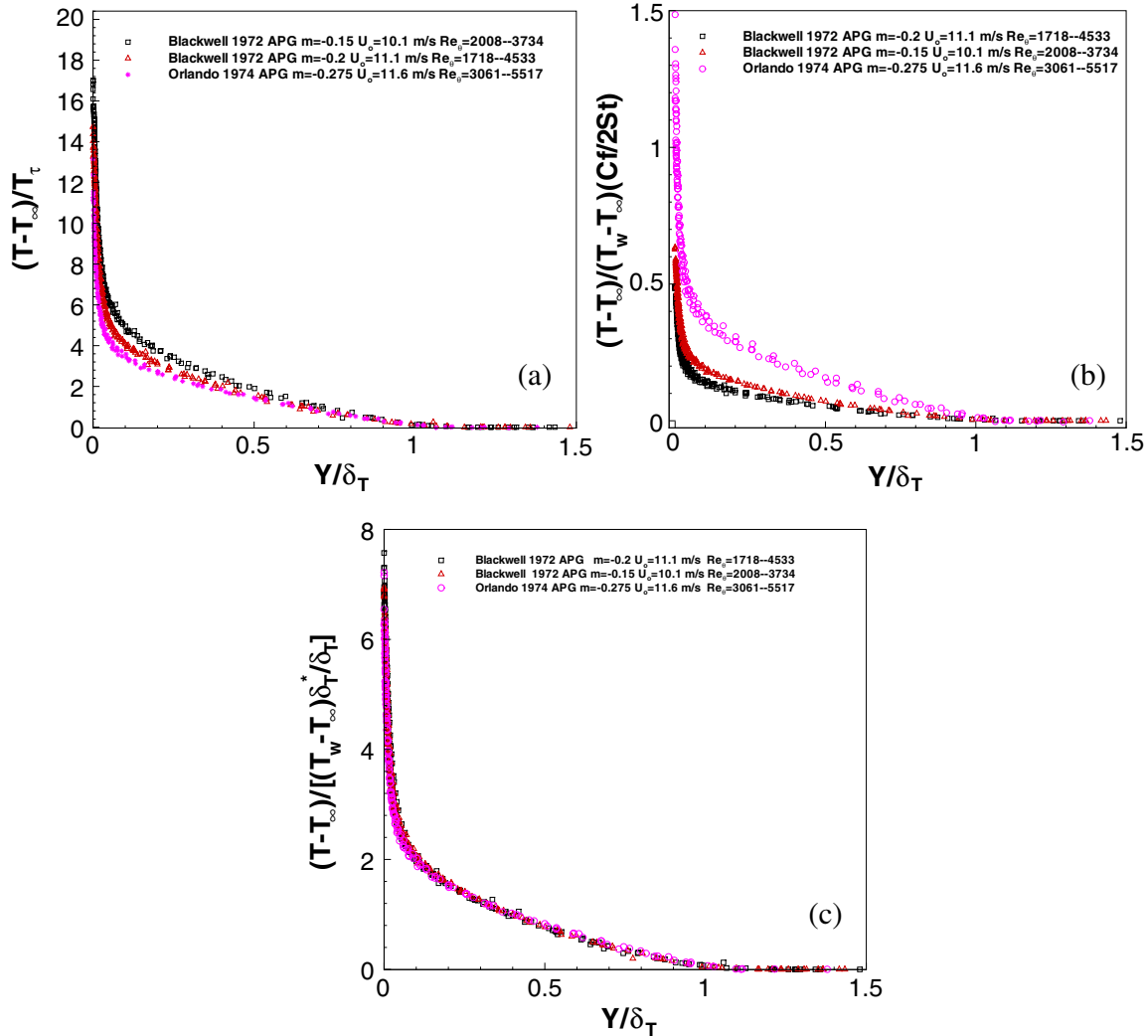


Figure 6. Comparisons of different outer scalings for the APG flow. (a) Scaling using Reynolds analogy. (b) Scaling using the GWC analysis. (c) Scaling from the present analysis.

Figure 7 shows the FPG experimental data from figure 3. Using the new scaling shown in figure 7(c), the data collapse better than using the classical scaling shown in figure 7(a) and the GWC scaling shown in figure 7(b).

Figure 8 shows the above ZPG, APG and FPG experimental data plotted together in outer variables. Evidently, all APG profiles collapse to the same curve, and all the FPG collapse to another curve. For the ZPG profile, the Blackwell ZPG profiles collapse to one curve, which is almost the same profile as the APG data. However, the Blom data collapse to a totally different curve from the Blackwell ZPG because of the unheated section. This unheated region has a direct influence on the outer flow but not on the inner flow as shown in figure 1(c), which further shows that the importance of the upstream conditions in the outer flow. The results shown here using

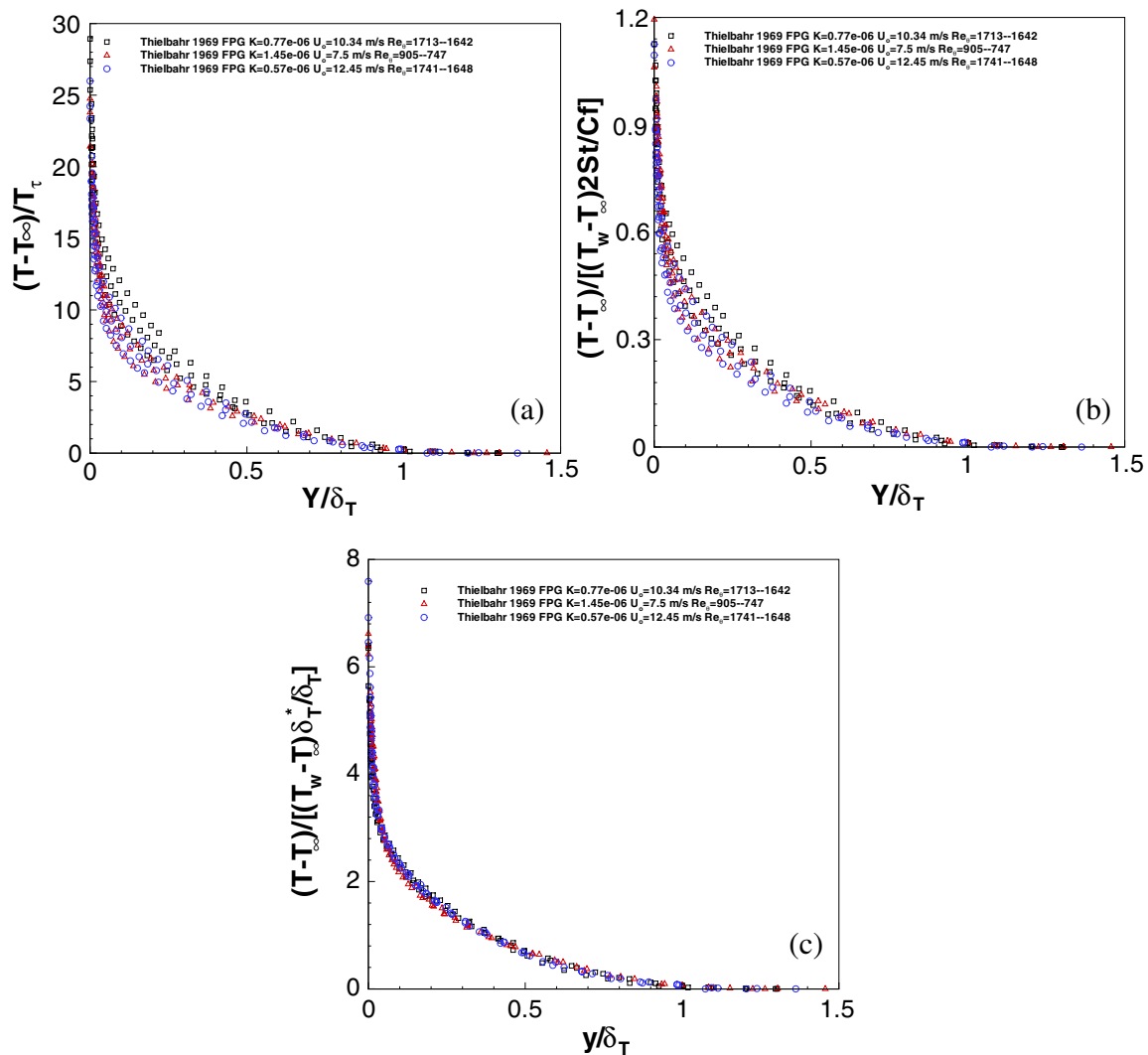


Figure 7. Comparisons of different outer scalings for the FPG flow. (a) Scaling using Reynolds analogy. (b) Scaling using the GWC analysis. (c) Scaling from the present analysis.

the classical scaling or the GWC scaling are consistent with the observations of Castillo and Walker [21]. They showed that the mean velocity deficit profiles normalized by U_∞ collapsed as long as the wind tunnel speed (upstream conditions) was kept fixed. However, each profile collapses to a different curve depending on the upstream conditions. They further showed that the Reynolds number dependence observed in the boundary layer was mainly due to changes in the upstream conditions. Notice that the new scaling removes the effect of the upstream conditions and the strength of PG in the boundary layer, contrary to the classical scaling. This result is consistent with the recent findings by Castillo and George [12], Castillo and Walker [21] and Walker and Castillo [22], which showed that there are only three velocity profiles in turbulent boundary layers: one for ZPG, one for FPG and one for APG.

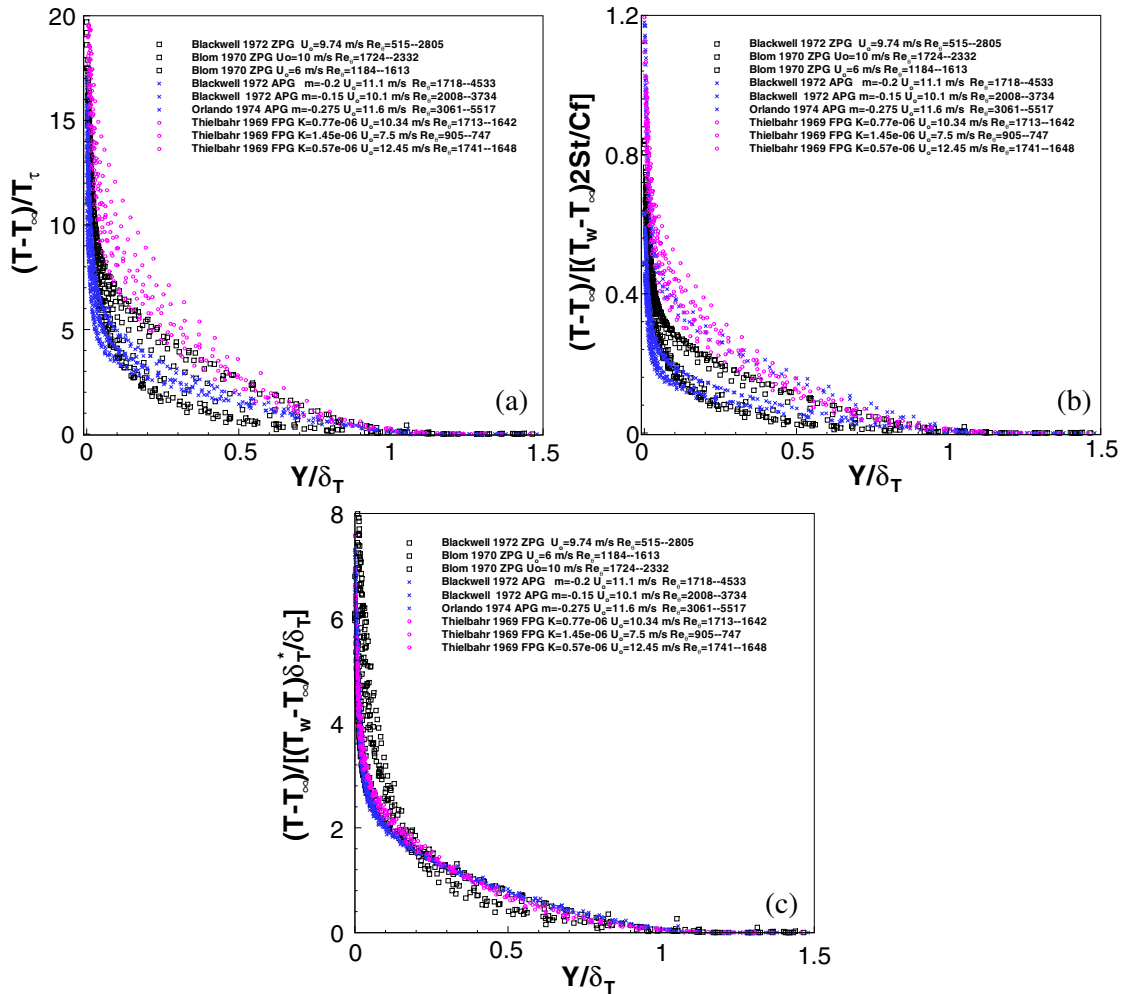


Figure 8. Comparisons of different outer scalings for the ZPG, APG and FPG flow. (a) Scaling using Reynolds analogy. (b) Scaling using the GWC analysis. (c) Scaling from the present analysis.

5. Conclusion

New inner and outer temperature scalings are derived for a 2D forced convection turbulent boundary layer subject to external PG using similarity analysis of the equations of motion. The new scalings were compared with the classical scaling and the GWC scaling.

It is shown that both the inner and outer flows are affected by the external PG and the upstream conditions such as the wind tunnel speed. However, when the experimental data are normalized by the new scaling in inner variables $T_{si} = Pr(T_w - T_\infty)\sqrt{St}$ or in outer variables $T_{so} = (T_w - T_\infty)\delta_T^*/\delta_T$, the effects of PG and upstream conditions are completely removed from the profiles. The fact that the inner profiles collapse to one single curve for all the ZPG, APG and FPG flows means that the inner flow is nearly independent of the PG, contrary to the outer flow where the shape of those profiles are different. Consequently, the external PG has more influence on the outer flow than on the inner flow.

Moreover, using the new scalings, the profiles collapse into a single curve; thus, the asymptotic profiles for the thermal boundary layer are found even at finite Reynolds number and finite Péclet number. In summary, the similarity analysis applied to forced convection boundary layers enables us to find the true asymptotic solutions in thermal boundary layers, and it provides new insight into the effects of the upstream conditions and PG on the downstream flow.

Acknowledgments

The authors are very thankful to Dr William St Cyr and Dr Ramona Travis from NASA Stennis Space Center for their continuous support of many of our projects.

References

- [1] Zagarola M V and Smits A J 1998 Mean-flow scaling of turbulent pipe flow *J. Fluid Mech.* **373** 33–79
- [2] Kader B A 1991 Heat and mass transfer in pressure-gradient boundary layers *Int. J. Heat Mass Transfer* **34** 2837–57
- [3] Spalding D B 1961 A single formula for the 'law of the wall' *Trans. ASME, J. Appl. Mech.* **28** 455–8
- [4] Blackwell B F, Kays W M and Moffat R J 1972 The turbulent boundary layer on a porous plate: an experimental study of the heat transfer behavior with adverse pressure gradients *Report No HMT-16* Thermosciences Division, Department of Mechanical Engineering, Stanford University (*PhD Thesis*)
- [5] Ayala A, White B R and Bagheri N 1997 Turbulent Prandtl number measurements in adverse pressure gradient equilibrium boundary layers *2nd Int. Symp. on Turbulence, Heat and Mass Transfer* (Delft: Delft University Press) pp 137–46
- [6] Monin A S and Yaglom A M 1971 *Statistic Fluid Mechanics* (Cambridge, MA: MIT Press)
- [7] Perry A E, Bell J B and Joubert P N 1966 Velocity and temperature profiles in adverse pressure gradient turbulent boundary layers *J. Fluid Mech.* **25** 299–320
- [8] Perry A E and Hoffmann P H 1976 An experimental study of turbulent convective heat transfer from a flat plate *J. Fluid Mech.* **77** 355–68
- [9] Volino R J and Simon T W 1997 Velocity and temperature profiles in turbulent boundary layer flows experiencing streamwise pressure gradients *J. Heat Transfer* **119** 433–9
- [10] George W K, Wosnik M and Castillo L 1997 Similarity analysis for forced convection thermal boundary layer *Transp. Phenomen. Thermal Sci. Process Eng.* **1** 239–44
- [11] George W K and Castillo L 1997 Zero pressure gradient turbulent boundary layer *Appl. Mech. Rev.* **50** 689–729
- [12] Castillo L and George W K 2001 Similarity analysis for turbulent boundary layer with pressure gradient: outer flow *AIAA J.* **39** 41–7
- [13] Tennekes H and Lumley J L 1972 *A First Course in Turbulence* (Cambridge, MA: MIT Press)
- [14] Kays W M and Crawford M E 1993 *Convective Heat and Mass Transfer* (New York: McGraw-Hill)
- [15] Castillo L 2000 Application of Zagarola/Smits scaling in turbulent boundary layers with pressure gradient *Advances in Fluids Mechanics (Montreal, Canada, May 2000)* vol 3, ed M Rahman and C A Brebbia pp 275–88
- [16] Blom J 1970 An experimental determination of the turbulent Prandtl number in a developing temperature boundary layer *PhD Thesis* Technische Hogeschool, Eindhoven, The Netherlands
- [17] Orlando A F, Kays W M and Moffat R J 1974 Turbulent transport of heat and momentum in a boundary layer subject to deceleration, suction, and variable wall temperature *Report No HMT-17* Thermosciences Division, Department of Mechanical Engineering, Stanford University
- [18] Thielbahr W H, Kays W M and Moffat R J 1969 The turbulent boundary layer: experimental heat transfer with strong favorable pressure gradients and blowing *Report No HMT-5* Thermosciences Division, Department of Mechanical Engineering, Stanford University
- [19] Castillo L 1997 Similarity analysis of turbulent boundary layers *PhD Dissertation* Department of Mechanical and Aerospace Engineering, SUNY/Bufalo, NY
- [20] Julien H L 1969 The turbulent boundary layer on a porous plate: experimental study of the effects of a favorable pressure gradient *Report No HMT-4* Thermosciences Division, Department of Mechanical Engineering, Stanford University
- [21] Castillo L and Walker D 2002 The effect of the upstream conditions on the outer flow of turbulent boundary layers *AIAA J.* **40** 1292–9
- [22] Walker D and Castillo L 2002 Effect of the upstream conditions on turbulent boundary layers *AIAA J.* **40** 2540–2